Proceedings

Drone polariscopy - towards remote sensing applications

Soon Hock Ng [1]*, Blake Allan [2], Daniel Ierodiaconou [2], Vijayakumar Anand [1], Alexander Babanin [3] and Saulius Juodkazis[1,4]*

[1] Optical Sciences Centre and ARC Training Centre in Surface Engineering for Advanced Materials (SEAM), School of Science, Computing and Engineering Technologies, Swinburne University of Technology, Hawthorn, Vic 3122, Australia
[2] School of Life and Environmental Sciences, Faculty of Science Engineering & Built Environment, Deakin University, Princes Highway, Warrnambool, Victoria 3280, Australia
[3] Department of Infrastructure Engineering, University of Melbourne, VIC 3010, Australia
[4] World Research Hub Initiative (WRHI), School of Materials and Chemical Technology, Tokyo Institute of Technology, 2-12-1, Ookayama, Meguro-ku, Tokyo 152-8550, Japan.
* Correspondence: soonhockng@swin.edu.au (S.H.N); saulius.juodkazis@gmail.com (S.J.)

Abstract: Remote sensing is critical for a wide range of applications, including ocean and wave monitoring, planetary exploration, agriculture, and astronomy. We demonstrated a polariscopy concept which is able to determine orientation of patterns below the optical resolution limit of a system. This technique relies on measuring at least 4 different polarisation angles and calculating the orientation from the set of intensity information. It was initially demonstrated on the infrared microspectroscopy beamline at the Australian Synchrotron using IR light in transmission. Using a monochrome polarising camera, it was shown that it also worked in optical transmission. This camera was mounted onto a drone as a remote sensing platform and orientation information was extracted from reflection images taken at an altitude where conventional imaging could not resolve the test patterns. In the interest of moving towards high-speed data acquisition and processing, two methods for processing the image are compared – an analytical and curve fitting method.

Keywords: Polariscopy; remote sensing; drone; image processing

Citation: Lastname, F.; Lastname, F.; Lastname, F. Drone polariscopy - towards remote sensing applications. *Proceedings* **2021**, *1*, 0. https://doi.org/

Published:

1. Introduction

The ability to detect periodic features below the resolution limit of a system is valuable to all forms of imaging. This is especially important in areas such as remote sensing where the cost of launching a satellite is dependent on its mass. Polarisation information adds an additional dimension to image data and has shown value in machine vision where it is utilised for analysis of reflections [1]. However in such a context, it has not been used for diffraction limited imaging of anisotropy. A method using Fourier Transform infrared spectroscopy was developed and transferred to the Infrared Microspectroscopy beamline at the Australian Synchrotron which demonstrated anisotropy recognition and mapping below the spatial resolution limit for the first time [2,3]. The method described – the 4-pol method – involves measuring the sample at 4 polarisation angles (0°, 45°, 90°, and 135° (-45°)). In addition to molecular anisotropy, the orientation of a circular grating with a 200 nm pitch and 100 nm line width was detectable with a system resolution of 5 μm, a 25$\times$ difference [4]. To demonstrate the ability of the 4-pol method to move beyond the IR wavelengths and microscopy scale, a 4-pol visible light camera was used to show orientation detection in the visible wavelength range [5]. Here we extend the method even further and mount the camera on a drone which functions as a remote sensing platform analogue and operates in reflection mode.

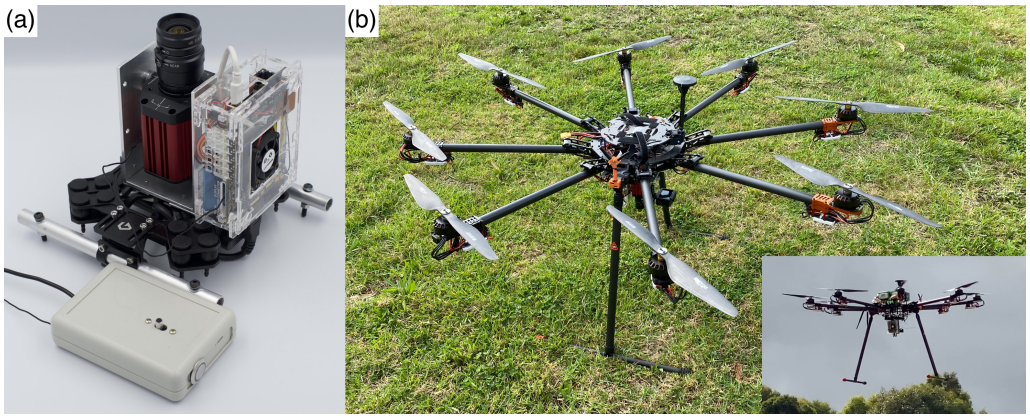

Figure 1. (**a**) Photograph of the polarisation camera in it's mounting rig along with a remote control. (**b**) Preflight photo of the octocopter with camera module attached underneath. Inset shows the drone and camera just after takeoff.

2. Materials and Methods

2.1. Drone Flight with Polarisation Camera

The CS505MUP monochrome polarisation camera (Thorlabs Inc.) has a 2448×2048 pixel sensor with micro-polarisers directly over each pixel. Each 2×2 group of pixels provides 0°, 45°, 90°, and 135° intensity information for a total of 1224×1024 for each polarisation angle. The camera was attached to a custom mounting rig which provided vibration damping, battery, LattePanda computer with receiver, and a GoPro video camera (Figure 1a). This rig was then bolted under a Kraken 130V2 octocopter drone platform (Figure 1b). After takeoff, the acquisition was remotely triggered to conserve power as well as storage space. To account for different lighting conditions, the camera was programmed to record a bursts of 10 images at varying exposure times, every 30 s. The drone was flown up in steps of 20 m and hovered for 1 min to ensure a full set of images were acquired at each altitude. 3D printed targets (Figure 2) consisting of 0.5 mm lines with a 1 mm pitch (one circular with an Archimedean spiral and one rectangular with different orientations in each quadrant) were set up on the ground as points of known orientation. The diameter of the circle was 20 cm and the dimensions of the rectangle were 24×20 cm

2.2. Data Processing

The data was subsequently converted to intensity and orientation information using two methods – analytical and curve fitting [2,6]. For the analytical solution, the intensity is given by

$$I = \frac{I_{0^\circ} + I_{45^\circ} + I_{90^\circ} + I_{135^\circ}}{2}, \tag{1}$$

where I is the image intensity and I_{θ° is the intensity at a specific polarisation angle. The orientation (azimuth) is given by

$$\psi = \frac{1}{2}\arctan2\left(\frac{I_{45^\circ} - I_{135^\circ}}{I_{0^\circ} - I_{90^\circ}}\right), \tag{2}$$

where arctan2 is the four quadrant inverse tangent. The equation used for fitting was

$$I(\theta) = A\cos(2\theta - 2\psi) + c, \tag{3}$$

where $I(\theta)$ is the intensity at a specific polariser angle, A is a factor proportional to the degree of polarisation, θ the polariser angle, ψ the azimuth, and c as a factor proportional to I. The bounds of the fit were $0 < A < 5$, $-\frac{\pi}{2} < \psi < \frac{\pi}{2}$, and $-5 < c < 5$ with an initial guess of $A = 1$, $\psi = 0$, and $c = 1$. In all cases, these were the values used for all pixels.

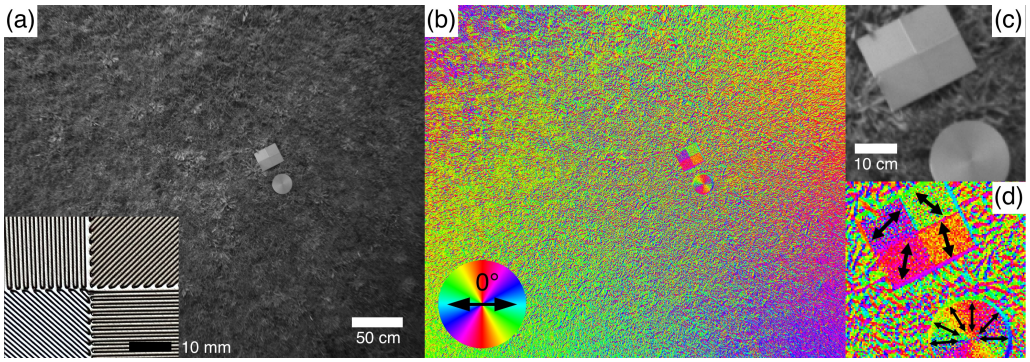

Figure 2. (**a**) Intensity image of 3D printed targets on a grass field at an altitude of ∼4 m. Inset shows a photo of the centre of the rectangular target showing the orientation in each quadrant. (**b**) Corresponding azimuth map with the colours indicating azimuth angle. (**c**) Enlarged intensity image of the targets. (**d**) Enlarged azimuth image of the targets with black arrows indicating approximate calculated azimuth orientation.

3. Results and Discussion

3.1. Orientation Determination

Figure 2a shows an intensity image, calculated with Equation 1, at an altitude of approximately 4 m and the inset shows a photo of 3D printed lines on the rectangular target. This height is equivalent to 3 pixels/cm in the image or 6 pixels/cm over the full sensor (calculated using the 20 cm diameter circle as reference). Since the spacing between the lines are 0.5 mm, the lines are not resolved in the image. Applying Equation 2 results in Figure 2b which shows colours representing the azimuth angle with 0° defined as shown in the bottom left. It's evident that each quadrant of the rectangular target shows a different orientation while the circular target shows radial changes. Figures 2c and 2d show enlarged versions of the region of interest with arrows in Figure 2d showing approximate azimuth orientation. The azimuth is orthogonal to the orientation of the printed lines for both rectangular and circular targets. This is in contrast to transmission mode where the calculated azimuth is parallel to the alignment [4]. However, the fact that the azimuth is consistent still indicates that the 4-pol method detects orientation that cannot be resolved by the optics in reflection. It also shows that it works in cases where either the detected features are much smaller or much larger than the wavelength of the probing light. The difference is azimuth alignment might be due to the illumination from the sky since polarisation varies with angle from the sun [7].

3.2. Data Processing Method

There are cases where there is low signal to noise, the angle of a polariser cannot be set precisely, or where the polarisation combinations are not 45° apart. The analytical method cannot accommodate these and so curve fitting can be used to determine the azimuth and intensity. This comes at a time cost however. While Equations 1 and 2 can be vectorised so the calculation can be performed on an entire image at once, curve fitting needs to be done for each pixel. As a single thread process, the analytical method takes < 1 s to process 1 frame. The same frame using curve fitting takes over 3 hours.

While the fitting method is slow, it ultimately returns the very similar results to the analytical method, when the bounds are set correctly. Figure 3a shows an enlarged crop from Figure 2b and Figure 3b shows the same area but calculated by fitting each pixel. At a glance, they are indistinguishable however Figure 3c shows that there are several pixels which are different. These differences are not very significant as the proportion of pixels that don't agree are few. The time disparity demonstrates that the fitting method should only be used when a greater number of polarisation measurements are needed – the case where signal to noise is low.

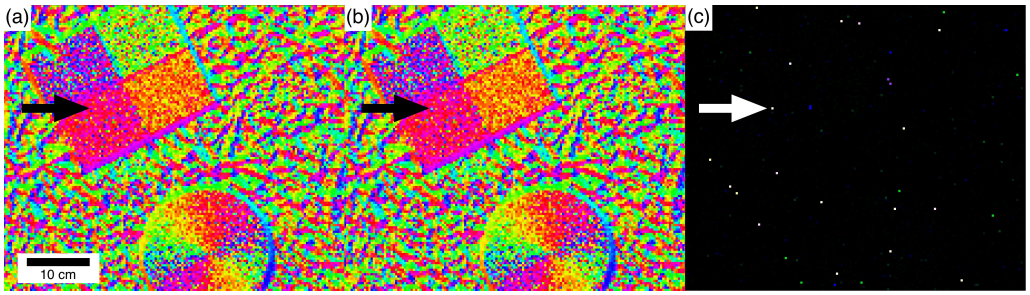

Figure 3. (**a**) Azimuth image calculated using Equation 2 (**b**) Azimuth image calculated by fitting Equation 3. (**c**) Images **a** and **b** overlaid with the difference image blend mode showing pixels that are different as a colour and pixels which are the same as black. Arrows are eye guides to one pixel which is different.

4. Conclusions

The 4-pol method was successfully transferred from the infrared microspectroscopy beamline to a drone platform. It was shown that orientation could be determined even when the aligned features could not be spatially resolved. The calculated azimuth was orthogonal to the alignment direction and the reason for this requires further study. This is stepping stone towards satellite-based remote sensing using the technique and opens up possibilities for ocean monitoring, planetary observation, and astronomy where orientation information is important.

Author Contributions: Conceptualization, S.J. and S.H.N.; methodology, S.H.N.; software, S.H.N., V.A.; investigation, S.H.N., B.A., D.I., V.A., A.B., S.J.; resources, B.A., D.I., A.B.; data curation, S.H.N.; writing—original draft preparation, S.H.N., S.J.; writing—review and editing, S.H.N., S.J., B.A, D.I., and V.A.; visualization, S.H.N.; supervision, D.I., A.B., and S.J. All authors have read and agreed to the published version of the manuscript.

Funding: This research was funded by the Australian Research Council grant number LP190100505.

Data Availability Statement: The data presented in this study are available on request from the corresponding author.

Conflicts of Interest: The authors declare no conflict of interest.

References

1. Atkinson, G.A.; Ernst, J.D. High-sensitivity analysis of polarization by surface reflection. *Machine Vision and Applications* **2018**, *29*, 1171–1189. doi:10.1007/s00138-018-0962-7.
2. Hikima, Y.; Morikawa, J.; Hashimoto, T. FT-IR Image Processing Algorithms for In-Plane Orientation Function and Azimuth Angle of Uniaxially Drawn Polyethylene Composite Film. *Macromolecules* **2011**, *44*, 3950–3957. doi:10.1021/ma2003129.
3. Ryu, M.; Balčytis, A.; Wang, X.; Vongsvivut, J.; Hikima, Y.; Li, J.; Tobin, M.J.; Juodkazis, S.; Morikawa, J. Orientational Mapping Augmented Sub-Wavelength Hyper-Spectral Imaging of Silk. *Scientific Reports* **2017**, *7*, 1–10. doi:10.1038/s41598-017-07502-3.
4. Honda, R.; Ryu, M.; Moritake, M.; Balčytis, A.; Mizeikis, V.; Vongsvivut, J.; Tobin, M.J.; Appadoo, D.; Li, J.L.; Ng, S.H.; Juodkazis, S.; Morikawa, J. Infrared Polariscopy Imaging of Linear Polymeric Patterns with a Focal Plane Array. *Nanomaterials* **2019**, *9*, 732. doi:10.3390/nano9050732.
5. Ng, S.H.; Anand, V.; Duffy, A.; Babanin, A.; Ryu, M.; Morikawa, J.; Juodkazis, S. Remote-sensing concept using polariscopy for orientation determination below the spatial resolution limit. Photonic Instrumentation Engineering VIII; Soskind, Y.; Busse, L.E., Eds. SPIE, 2021, Vol. 1169306, p. 4. doi:10.1117/12.2577096.
6. Ryu, M.; Nishijima, Y.; Morimoto, S.; To, N.; Hashizume, T.; Matsubara, R.; Kubono, A.; Hu, J.; Ng, S.H.; Juodkazis, S.; Morikawa, J. Hyperspectral Molecular Orientation Mapping in Metamaterials. *Applied Sciences* **2021**, *11*, 1544. doi:10.3390/app11041544.
7. Coulson, K.L. *Polarization and intensity of light in the atmosphere*; A. Deepak: Hampton Va, USA, 1988.